Electronic Supplementary Information

Luminescence tuning and single-phase white light emitters based on rare earth ions doped into a bismuth coordination network

C. S. Cunha,[a,b] M. Köppen,[b] H. Terraschke,[b] G. Friedrichs,[c] O. L. Malta[d], N. Stock[b] and H. F. Brito[a]

[a]Institute of Chemistry, University of São Paulo, Av. Prof. Lineu Prestes, 748, 05508-000, São Paulo – SP, Brazil

[b]Institute of Inorganic Chemistry, University of Kiel, Max-Eyth Straße 2, 24118 Kiel, Germany

[c]Institute of Physical Chemistry, University of Kiel, Max-Eyth Straße, 1, 24118 Kiel, Germany

[d]Department of Fundamental Chemistry, Federal University of Pernambuco, Av. Prof. Moraes Rego, 1235, 50670-901, Recife – PE, Brazil

*Corresponding Author, e-mail: hefbrito@iq.usp.br.

Table of Contents

1. Experimental section

Table S1. Molar ratios, masses of $Bi(NO_3)_3 \cdot 5H_2O$, H_4Pyr linker and volumes of solvent and $RE(NO_3)_3$ 0.05 M aqueous solution (RE^{3+}: Sm^{3+}, Eu^{3+}, Tb^{3+} and Dy^{3+}) for the up-scaled samples.

Samples	Molar ratio linker:metal		Dop.1 %	Dop.2 %	H_4Pyr mg	H_2O µL	Bi mg	Dop1 µL	Dop2 µL
Nondoped	1.0	0.3	0.0	0.0	250.0	10000	143.1	0	0
Eu^{3+}	1.0	0.3	5.0	0.0	250.0	9705	136.0	295	0
Tb^{3+}	1.0	0.3	5.0	0.0	250.0	9705	136.0	295	0
Dy^{3+}	1.0	0.3	5.0	0.0	250.0	9705	136.0	295	0
Sm^{3+}	1.0	0.3	5.0	0.0	250.0	9705	136.0	295	0
Tb^{3+}:Eu^{3+}	1.0	0.3	4.0	1.0	250.0	9705	136.0	236	59
Tb^{3+}:Sm^{3+}	1.0	0.3	1.0	4.0	250.0	9705	136.0	59	236
Dy^{3+}:Eu^{3+}	1.0	0.3	4.4	0.6	250.0	9705	136.0	260	35
Dy^{3+}:Eu^{3+}	1.0	0.3	4.6	0.4	250.0	9705	136.0	271	24
Dy^{3+}:Eu^{3+}	1.0	0.3	4.7	0.3	250.0	9705	136.0	277	18
Dy^{3+}:Sm^{3+}	1.0	0.3	2.0	3.0	250.0	9705	136.0	118	177
Dy^{3+}:Sm^{3+}	1.0	0.3	1.0	4.0	250.0	9705	136.0	59	236

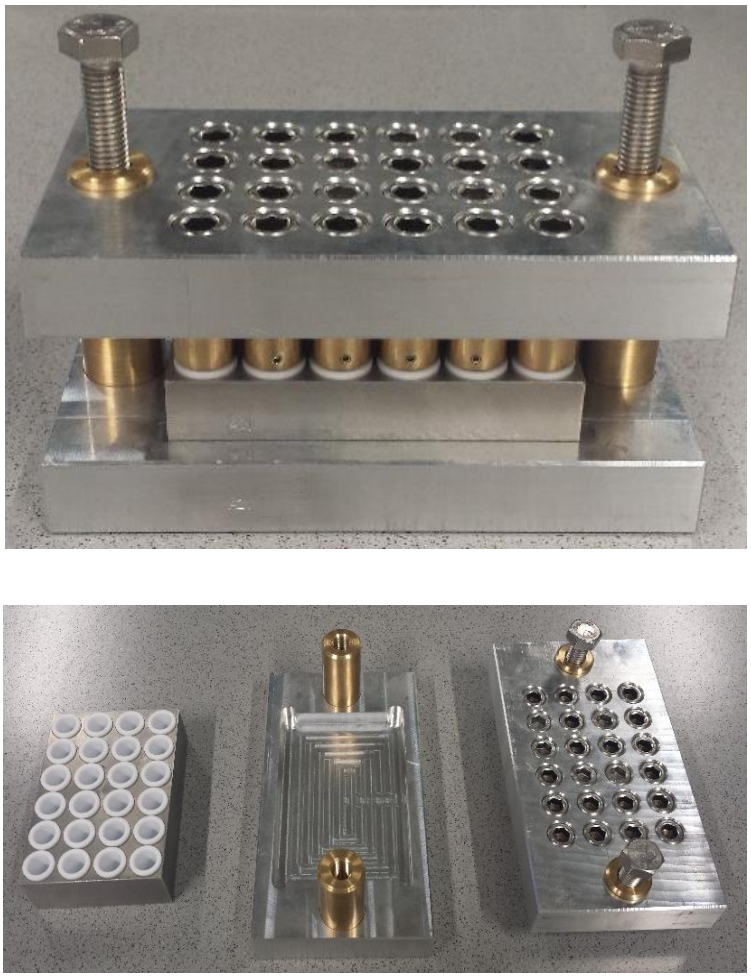

Fig. S1. Pictures of the closed (top) and opened (bottom) high-throughput hydrothermal reactor.

Table S2. Molar ratios, masses of $Bi(NO_3)_3 \cdot 5H_2O$, H_4Pyr linker and volumes of solvent and $RE(NO_3)_3$ 0.05 M aqueous solution (RE^{3+}: Eu^{3+} and Tb^{3+}) for the Tb^{3+}:Eu^{3+} double-doped [Bi(HPyr)].

Molar ratio		Tb^{3+}	Eu^{3+}	H_4Pyr	H_2O	Bi^{3+}	Tb^{3+}	Eu^{3+}
Linker : Metal		mol%	mol%	mg	µL	mg	µL	µL
1.0	0.3	5.0	0.0	25.0	970.5	13.6	29.5	0.0
1.0	0.3	4.7	0.3	25.0	970.5	13.6	27.7	1.8
1.0	0.3	4.5	0.5	25.0	970.5	13.6	26.6	3.0
1.0	0.3	4.2	0.8	25.0	970.5	13.6	24.8	4.7
1.0	0.3	4.0	1.0	25.0	970.5	13.6	23.6	5.9
1.0	0.3	3.7	1.3	25.0	970.5	13.6	21.8	7.7
1.0	0.3	3.5	1.5	25.0	970.5	13.6	20.7	8.9
1.0	0.3	3.2	1.8	25.0	970.5	13.6	18.9	10.6
1.0	0.3	3.0	2.0	25.0	970.5	13.6	17.7	11.8
1.0	0.3	2.7	2.3	25.0	970.5	13.6	15.9	13.6
1.0	0.3	2.5	2.5	25.0	970.5	13.6	14.8	14.8
1.0	0.3	2.2	2.8	25.0	970.5	13.6	13.0	16.5
1.0	0.3	2.0	3.0	25.0	970.5	13.6	11.8	17.7
1.0	0.3	1.7	3.3	25.0	970.5	13.6	10.0	19.5
1.0	0.3	1.5	3.5	25.0	970.5	13.6	8.9	20.7
1.0	0.3	1.2	3.8	25.0	970.5	13.6	7.1	22.4
1.0	0.3	1.0	4.0	25.0	970.5	13.6	5.9	23.6
1.0	0.3	0.7	4.3	25.0	970.5	13.6	4.1	25.4
1.0	0.3	0.5	4.5	25.0	970.5	13.6	3.0	26.6
1.0	0.3	0.3	4.7	25.0	970.5	13.6	1.8	27.7
1.0	0.3	0.0	5.0	25.0	970.5	13.6	0.0	29.5

Table S3. Molar ratios, masses of $Bi(NO_3)_3 \cdot 5H_2O$, H_4Pyr linker and volumes of solvent and $RE(NO_3)_3$ 0.05 M aqueous solution (RE^{3+}: Sm^{3+} and Tb^{3+}) for the Tb^{3+}:Sm^{3+} double-doped [Bi(HPyr)].

Molar ratio		Tb^{3+}	Sm^{3+}	H_4Pyr	H_2O	Bi^{3+}	Tb^{3+}	Sm^{3+}
Linker : Metal		mol%	mol%	mg	µL	mg	µL	µL
1.0	0.3	5.0	0.0	25.0	970.5	13.6	29.5	0.0
1.0	0.3	4.7	0.3	25.0	970.5	13.6	27.7	1.8
1.0	0.3	4.5	0.5	25.0	970.5	13.6	26.6	3.0
1.0	0.3	4.0	1.0	25.0	970.5	13.6	23.6	5.9
1.0	0.3	3.5	1.5	25.0	970.5	13.6	20.7	8.9
1.0	0.3	3.0	2.0	25.0	970.5	13.6	17.7	11.8
1.0	0.3	2.5	2.5	25.0	970.5	13.6	14.8	14.8
1.0	0.3	2.0	3.0	25.0	970.5	13.6	11.8	17.7
1.0	0.3	1.5	3.5	25.0	970.5	13.6	8.9	20.7
1.0	0.3	1.0	4.0	25.0	970.5	13.6	5.9	23.6
1.0	0.3	0.5	4.5	25.0	970.5	13.6	3.0	26.6
1.0	0.3	0.0	5.0	25.0	970.5	13.6	0.0	29.5

Table S4. Molar ratios, masses of $Bi(NO_3)_3 \cdot 5H_2O$, H_4Pyr linker and volumes of solvent and $RE(NO_3)_3$ 0.01 M aqueous solution (RE^{3+}: Dy^{3+} and Eu^{3+}) for the Dy^{3+}:Eu^{3+} double-doped [Bi(HPyr)].

Molar ratio		Dy^{3+}	Eu^{3+}	H_4Pyr	H_2O	Bi^{3+}	Dy^{3+}	Eu^{3+}
Linker	Metal	mol%	mol%	mg	µL	mg	µL	µL
1.0	0.3	4.95	0.05	25.0	852.4	13.6	146.1	1.5
1.0	0.3	4.90	0.10	25.0	852.4	13.6	144.6	3.0
1.0	0.3	4.85	0.15	25.0	852.4	13.6	143.1	4.4
1.0	0.3	4.80	0.20	25.0	852.4	13.6	141.6	5.9
1.0	0.3	4.75	0.25	25.0	852.4	13.6	140.2	7.4
1.0	0.3	4.70	0.30	25.0	852.4	13.6	138.7	8.9
1.0	0.3	4.65	0.35	25.0	852.4	13.6	137.2	10.3
1.0	0.3	4.60	0.40	25.0	852.4	13.6	135.7	11.8
1.0	0.3	4.55	0.45	25.0	852.4	13.6	134.3	13.3
1.0	0.3	4.50	0.50	25.0	852.4	13.6	132.8	14.8
1.0	0.3	4.45	0.55	25.0	852.4	13.6	131.3	16.2
1.0	0.3	4.40	0.60	25.0	852.4	13.6	129.8	17.7
1.0	0.3	4.35	0.65	25.0	852.4	13.6	128.4	19.2
1.0	0.3	4.30	0.70	25.0	852.4	13.6	126.9	20.7
1.0	0.3	4.20	0.80	25.0	852.4	13.6	123.9	23.6
1.0	0.3	4.10	0.90	25.0	852.4	13.6	121.0	26.6
1.0	0.3	4.00	1.00	25.0	852.4	13.6	118.0	29.5
1.0	0.3	3.90	1.10	25.0	852.4	13.6	115.1	32.5
1.0	0.3	3.80	1.20	25.0	852.4	13.6	112.1	35.4
1.0	0.3	3.70	1.30	25.0	852.4	13.6	109.2	38.4
1.0	0.3	3.60	1.40	25.0	852.4	13.6	106.2	41.3

Table S5. Molar ratios, masses of $Bi(NO_3)_3 \cdot 5H_2O$, H_4Pyr linker and volumes of solvent and $RE(NO_3)_3$ 0.05 M aqueous solution (RE^{3+}: Dy^{3+} and Sm^{3+}) for the Dy^{3+}:Sm^{3+} double-doped [Bi(HPyr)].

Molar ratio Linker : Metal		Dy^{3+} mol%	Sm^{3+} mol%	H_4Pyr mg	H_2O µL	Bi^{3+} mg	Dy^{3+} µL	Sm^{3+} µL
1.0	0.3	4.7	0.3	25.0	970.5	13.6	27.7	1.8
1.0	0.3	4.5	0.5	25.0	970.5	13.6	26.6	3.0
1.0	0.3	4.2	0.8	25.0	970.5	13.6	24.8	4.7
1.0	0.3	4.0	1.0	25.0	970.5	13.6	23.6	5.9
1.0	0.3	3.5	1.5	25.0	970.5	13.6	20.7	8.9
1.0	0.3	3.0	2.0	25.0	970.5	13.6	17.7	11.8
1.0	0.3	2.5	2.5	25.0	970.5	13.6	14.8	14.8
1.0	0.3	2.0	3.0	25.0	970.5	13.6	11.8	17.7
1.0	0.3	1.5	3.5	25.0	970.5	13.6	8.9	20.7
1.0	0.3	1.0	4.0	25.0	970.5	13.6	5.9	23.6
1.0	0.3	0.5	4.5	25.0	970.5	13.6	3.0	26.6
1.0	0.3	0.3	4.7	25.0	970.5	13.6	1.8	27.7

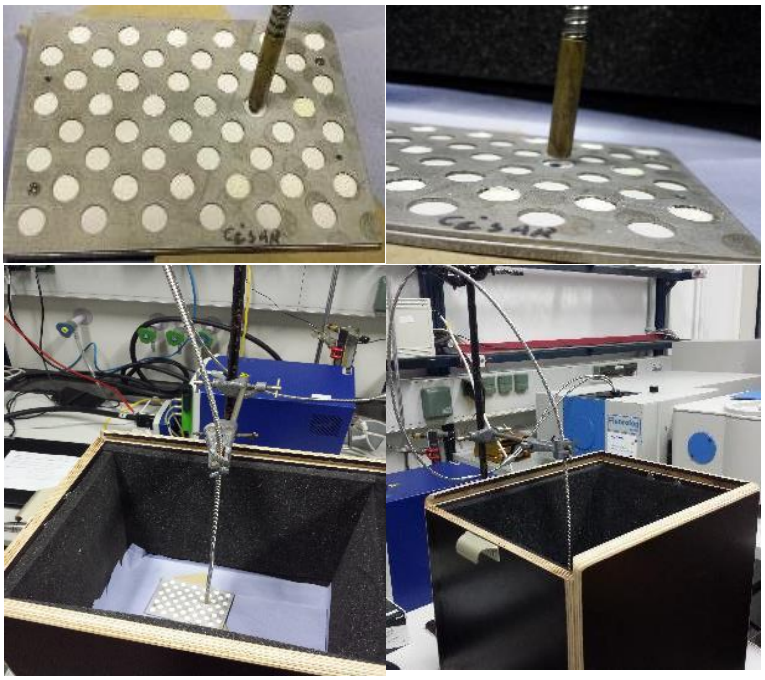

Fig. S2. Pictures of the optical fiber addressed to the high-throughput sample holder used to perform the photoluminescence measurements.

2. Doped [Bi(HPyr)] structural analysis

Table S6. Percentage of carbon and hydrogen calculated and found by elemental analysis of the up-scaled samples.

Sample	C %		H %	
	Found	Calc.	Found	Calc.
Nondoped [Bi(HPyr)]	26.1	26.1	0.6	0.7
Eu^{3+}(5.0 mol%)	26.5	26.3	0.6	0.7
Tb^{3+}(5.0)	26.3	26.3	0.6	0.7
Dy^{3+}(5.0)	26.3	26.2	0.5	0.7
Sm^{3+}(5.0)	26.5	26.3	0.7	0.7
Tb^{3+}(4.0):Eu^{3+}(1.0)	26.6	26.3	0.2	0.7
Tb^{3+}(1.0):Sm^{3+}(4.0)	26.3	26.3	0.5	0.7
Dy^{3+}(2.0):Sm^{3+}(3.0)	26.4	26.3	0.5	0.7
Dy^{3+}(4.7):Eu^{3+}(0.3)	26.5	26.2	0.6	0.7
Dy^{3+}(4.6):Eu^{3+}(0.4)	26.4	26.2	0.5	0.7
Dy^{3+}(4.4):Eu^{3+}(0.6)	26.4	26.2	0.5	0.7

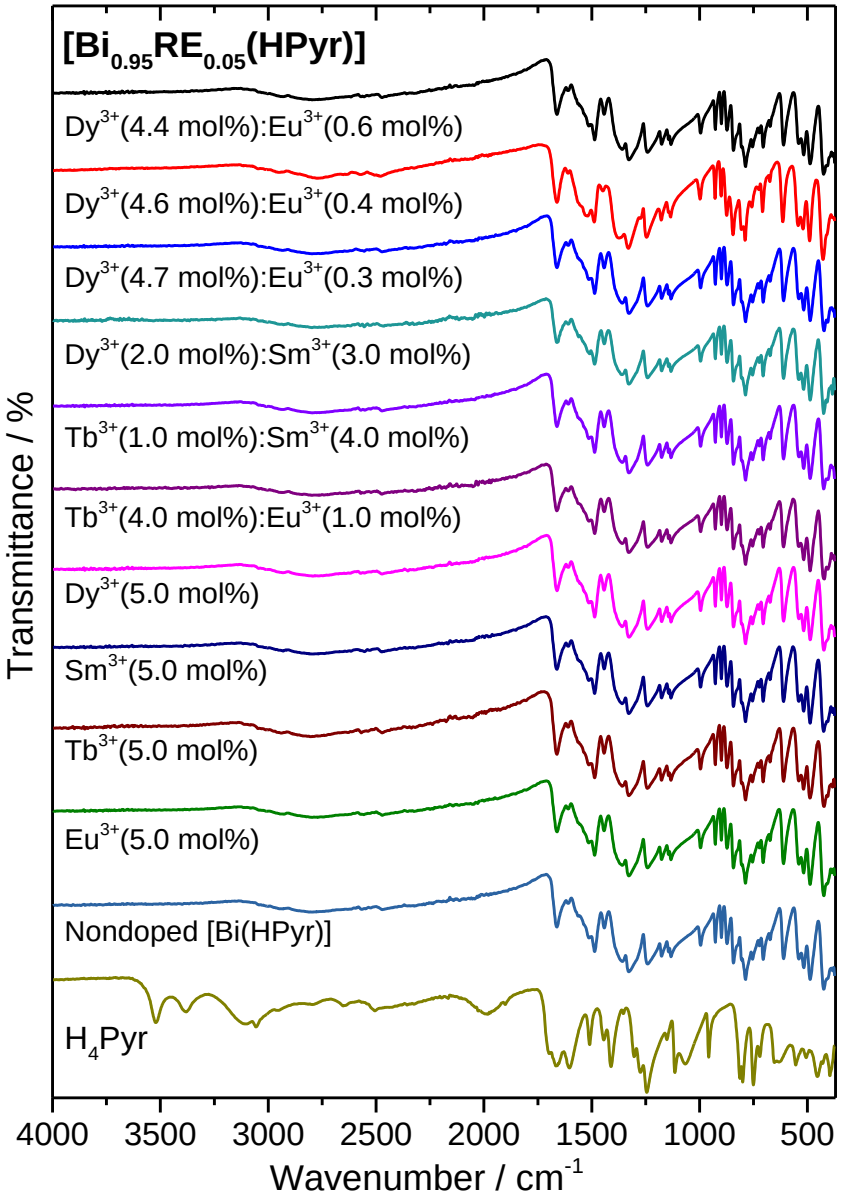

Fig. S3. IR spectra of the H_4Pyr linker and up-scaled nondoped and RE^{3+} doped [Bi(HPyr)] matrix.

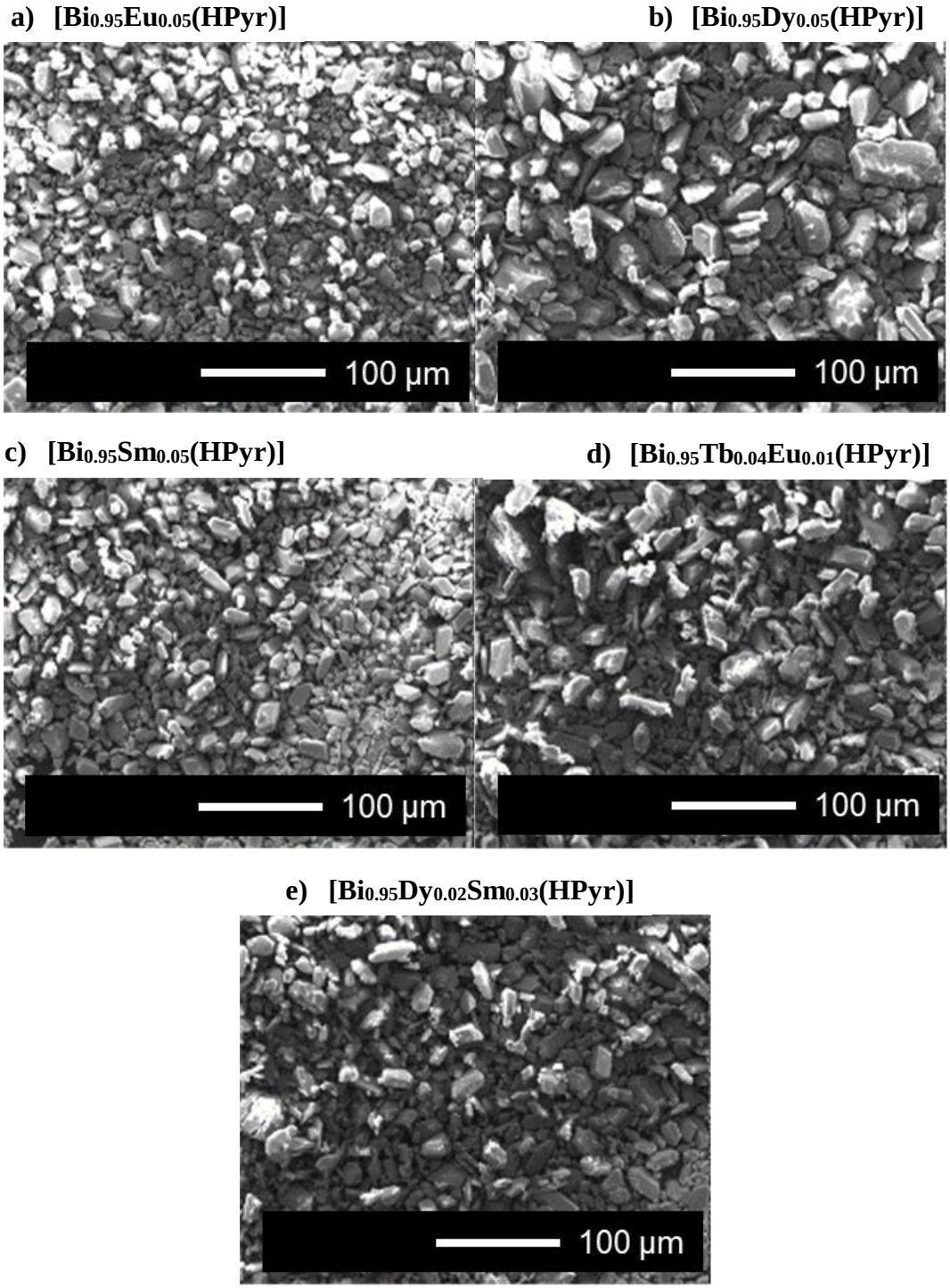

Fig. S4. SEM images of the RE^{3+} doped [Bi(HPyr)] materials: a) $[Bi_{0.95}Eu_{0.05}(HPyr)]$, b) $[Bi_{0.95}Dy_{0.05}(HPyr)]$, c) $[Bi_{0.95}Sm_{0.05}(HPyr)]$, d) $[Bi_{0.95}Tb_{0.04}Eu_{0.01}(HPyr)]$ and e) $[Bi_{0.95}Dy_{0.02}Sm_{0.03}(HPyr)]$.

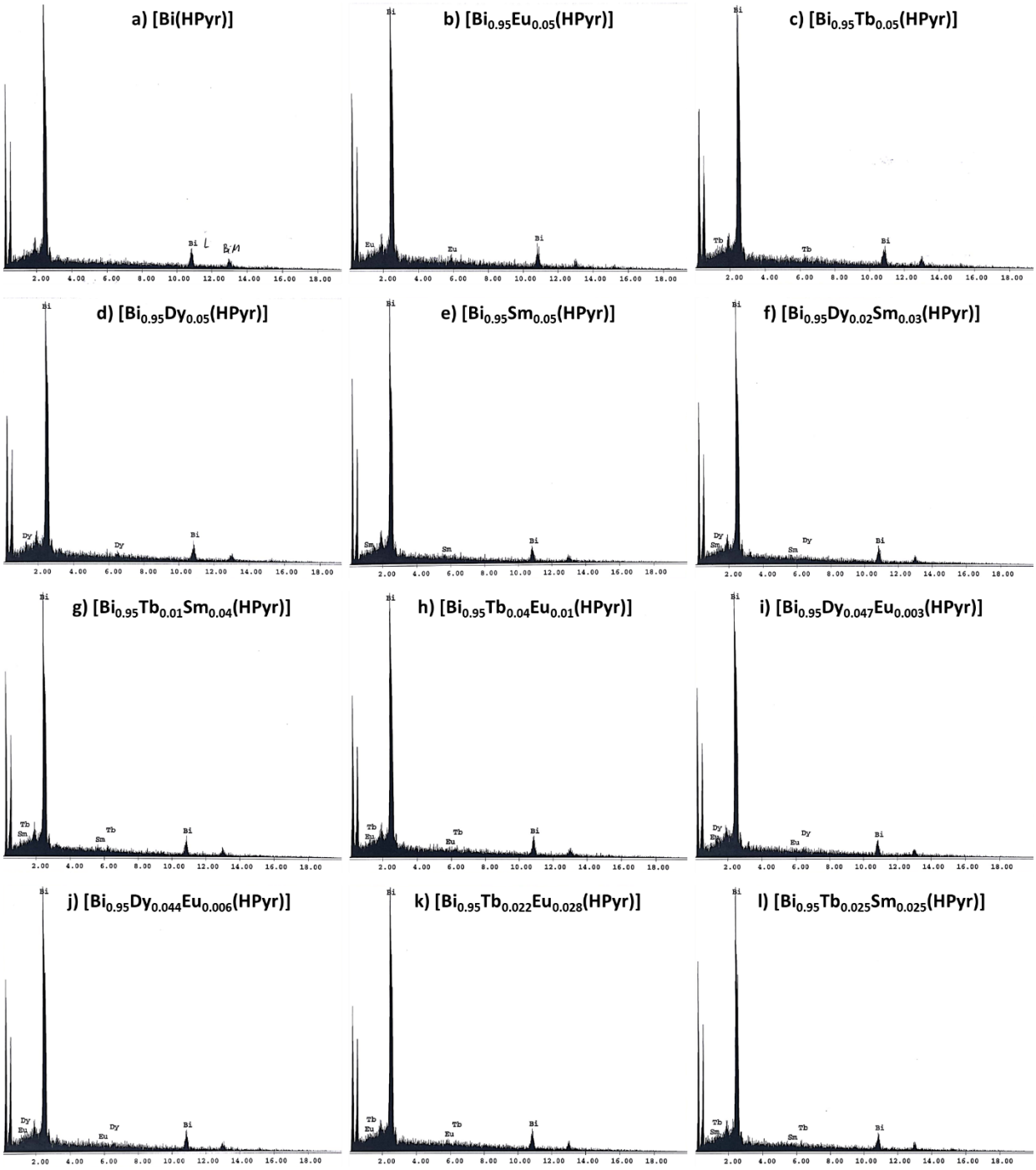

Fig. S5. The EDX spectra of the RE^{3+} doped [Bi(HPyr)] materials: a) nondoped matrix, b) $[Bi_{0.95}Eu_{0.05}(HPyr)]$, c) $[Bi_{0.95}Tb_{0.05}(HPyr)]$ d) $[Bi_{0.95}Dy_{0.05}(HPyr)]$, e) $[Bi_{0.95}Sm_{0.05}(HPyr)]$, f) $[Bi_{0.95}Dy_{0.02}Sm_{0.03}(HPyr)]$, g) $[Bi_{0.95}Tb_{0.01}Sm_{0.04}(HPyr)]$, h) $[Bi_{0.95}Tb_{0.04}Eu_{0.01}(HPyr)]$, i) $[Bi_{0.95}Dy_{0.047}Eu_{0.003}(HPyr)]$, j) $[Bi_{0.95}Dy_{0.044}Eu_{0.006}(HPyr)]$, k) $[Bi_{0.95}Tb_{0.022}Eu_{0.028}(HPyr)]$ and l) $[Bi_{0.95}Tb_{0.025}Sm_{0.025}(HPyr)]$.

Table S7. Bi^{3+} and RE^{3+} ions at. % obtained by EDX of the up-scaled [Bi(HPyr)] samples. Doping content of the samples is given in mol%.

[$Bi_{0.95}RE_{0.05}$(HPyr)]		Bi^{3+}	Dop. 1	Dop. 2
Dop 1	Dop 2	at. %	at. %	at. %
Eu^{3+}(5.0)		91.80	8.20	
Tb^{3+}(5.0)		94.25	5.75	
Dy^{3+}(5.0)		93.33	6.67	
Sm^{3+}(5.0)		94.14	5.86	
Dy^{3+}(2.0)	Sm^{3+}(3.0)	91.95	3.42	4.63
Tb^{3+}(1.0)	Sm^{3+}(4.0)	91.09	3.07	5.91
Tb^{3+}(4.0)	Eu^{3+}(1.0)	96.30	2.34	1.32
Dy^{3+}(4.7)	Eu^{3+}(0.3)	92.36	5.01	2.64
Dy^{3+}(4.4)	Eu^{3+}(0.6)	91.74	4.60	3.66
Tb^{3+}(2.2)	Eu^{3+}(2.8)	89.93	4.51	5.56
Tb^{3+}(2.5)	Sm^{3+}(2.5)	90.76	4.22	5.02

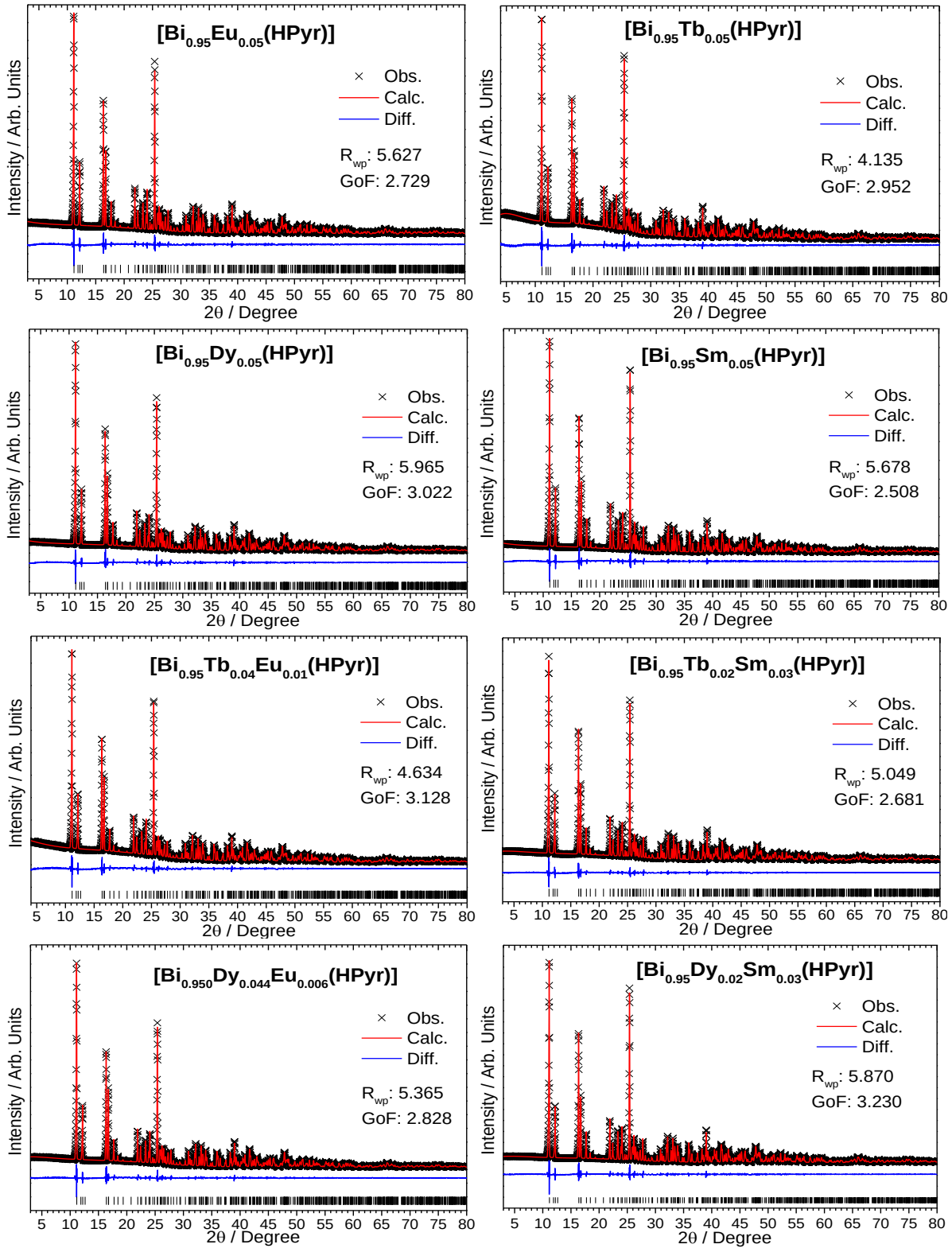

Fig. S6. Final plots of the LeBail fits of up-scaled RE^{3+} double-doped [Bi(HPyr)]. The observed powder patterns are shown in black, the calculated powder patterns as an overlay in red and the differences (observed minus calculated) of the two are given by lower blue lines. The allowed positions of the Bragg peaks are shown as tick marks.

Table S8. Unit cell parameters, volume, R_{wp} and GoF of the nondoped and RE^{3+} double-doped [Bi(HPyr)] materials. Doping content is given in mol%.

	[Bi(HPyr)]	Tb^{3+}(4.0) Eu^{3+}(1.0)	Tb^{3+}(2.0) Sm^{3+}(3.0)	Dy^{3+}(2.0) Sm^{3+}(3.0)	Dy^{3+}(4.4) Eu^{3+}(0.6)
R_{wp}	5.10	4.63	5.05	5.87	5.37
GoF	2.17	3.13	2.68	3.23	2.83
a / Å	7.27(1)	7.27(0)	7.26(9)	7.26(9)	7.26(7)
b / Å	8.16(4)	8.15(8)	8.15(7)	8.15(7)	8.15(6)
c / Å	8.64(4)	8.65(3)	8.65(2)	8.65(2)	8.65(1)
α / °	66.21(1)	66.17(2)	66.16(6)	66.16(4)	66.17(2)
β / °	86.58(8)	86.54(6)	86.54(4)	86.54(1)	86.54(5)
γ / °	84.52(2)	84.48(8)	84.48(8)	84.48(3)	84.48(6)
V / $Å^3$	467.3(2)	467.2(1)	466.9(9)	466.9(7)	466.8(4)

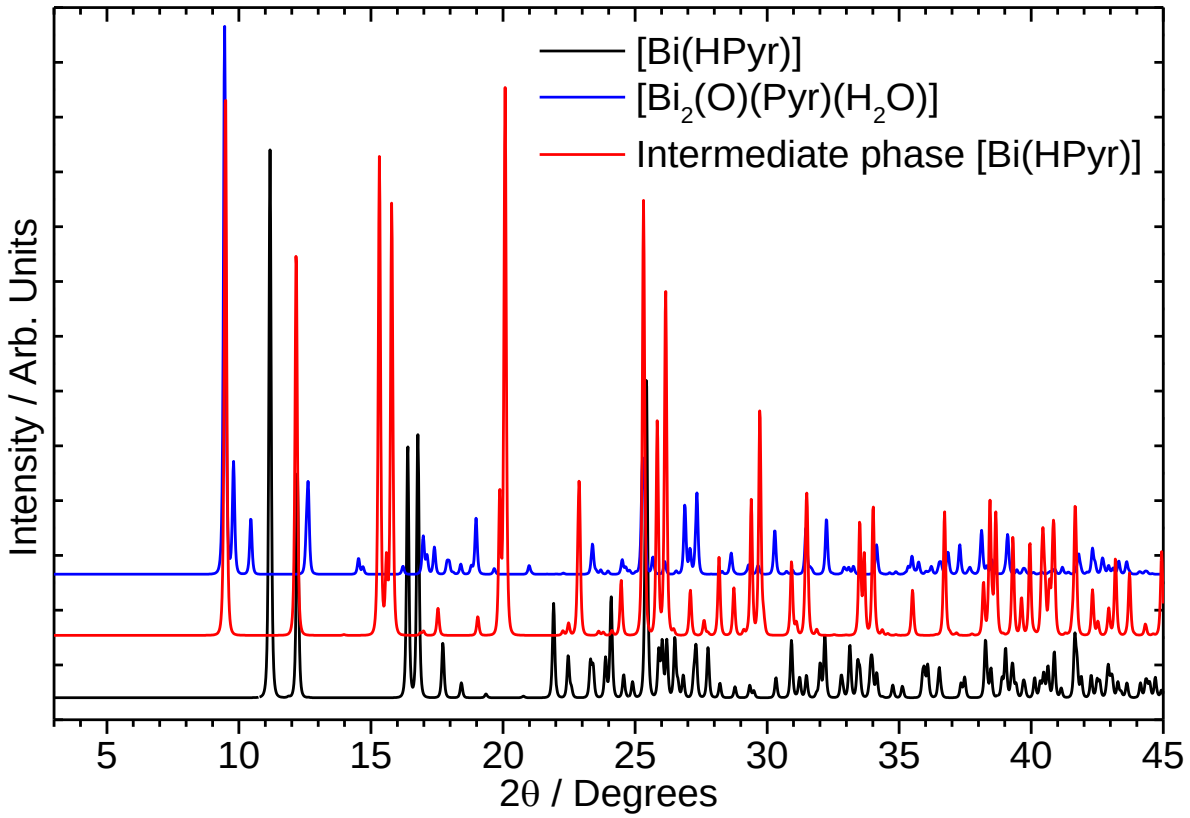

Fig. S7. Theoretical powder diffraction patterns of [Bi_2(O)(Pyr)(H_2O)] (blue line), intermediate phase (red line) and resultant [Bi(HPyr)] (black line).[1]

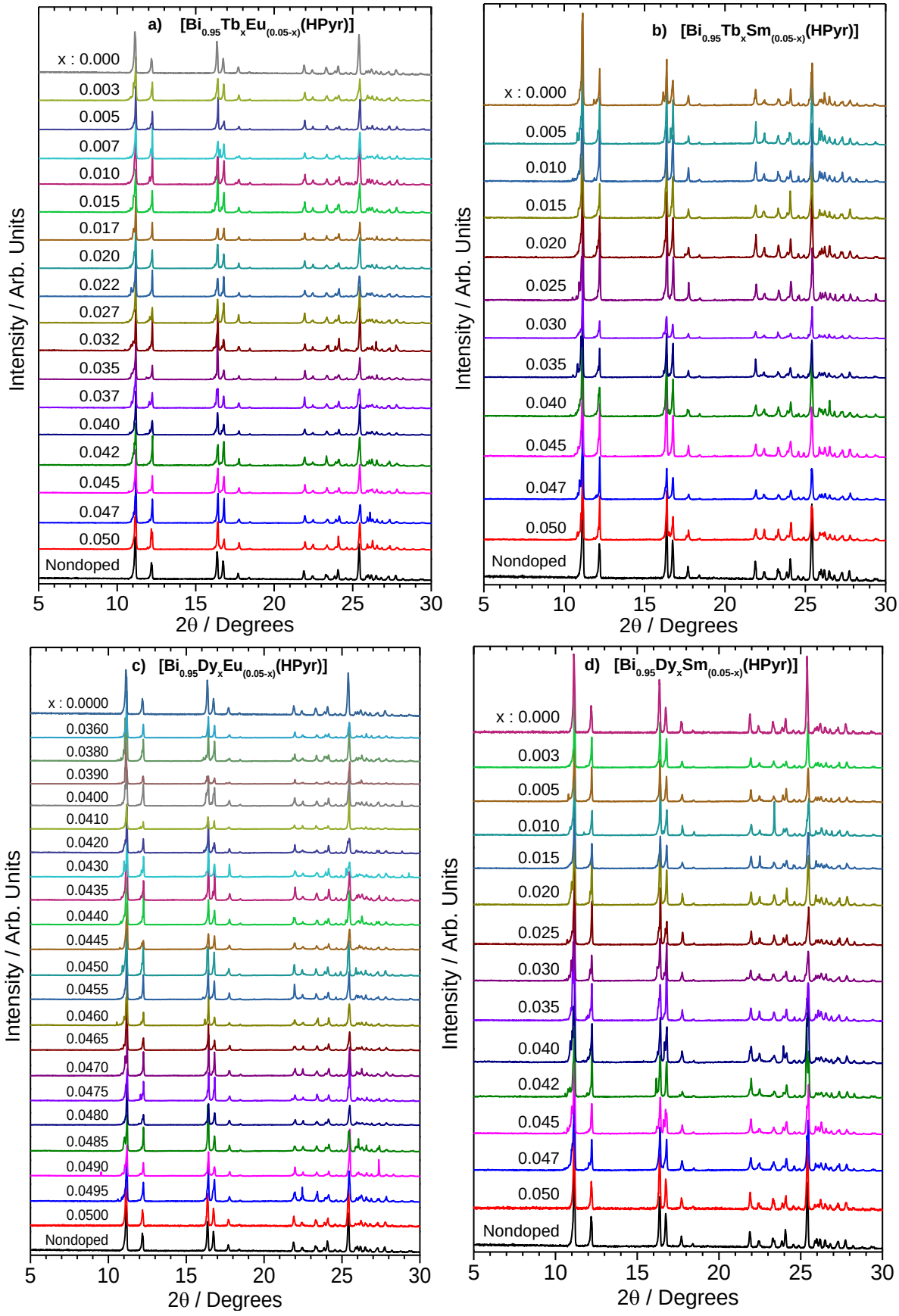

Fig. S8. PXRD patterns of the a) Tb^{3+}:Eu^{3+}, b) Tb^{3+}:Sm^{3+}, c) Dy^{3+}:Eu^{3+}, d) Dy^{3+}:Sm^{3+} double-doped [Bi(HPyr)] system.

3. Photoluminescence of the nondoped [Bi(HPyr)]

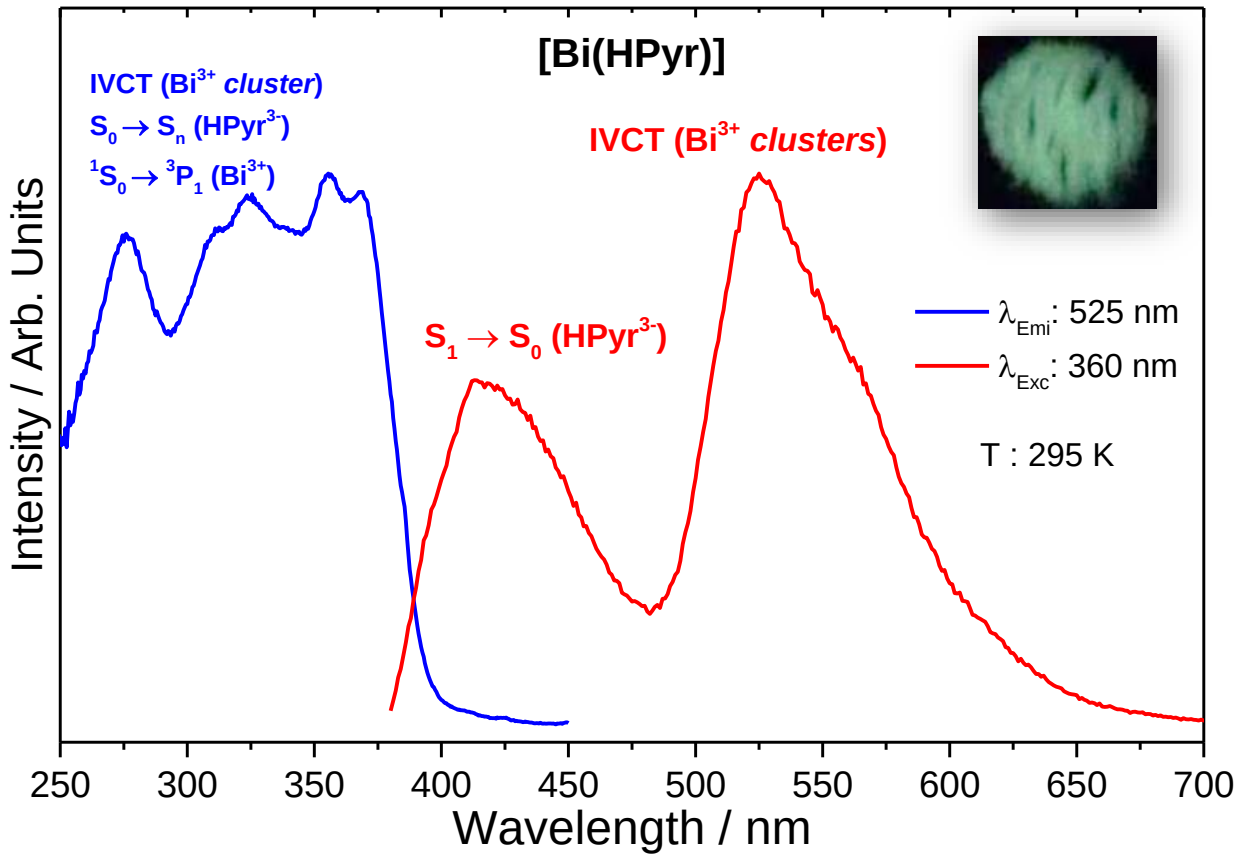

Fig. S9. Excitation (blue line, monitored at 525 nm) and emission spectra (red line, monitored at 360 nm) of nondoped [Bi(HPyr)] at 295 K.

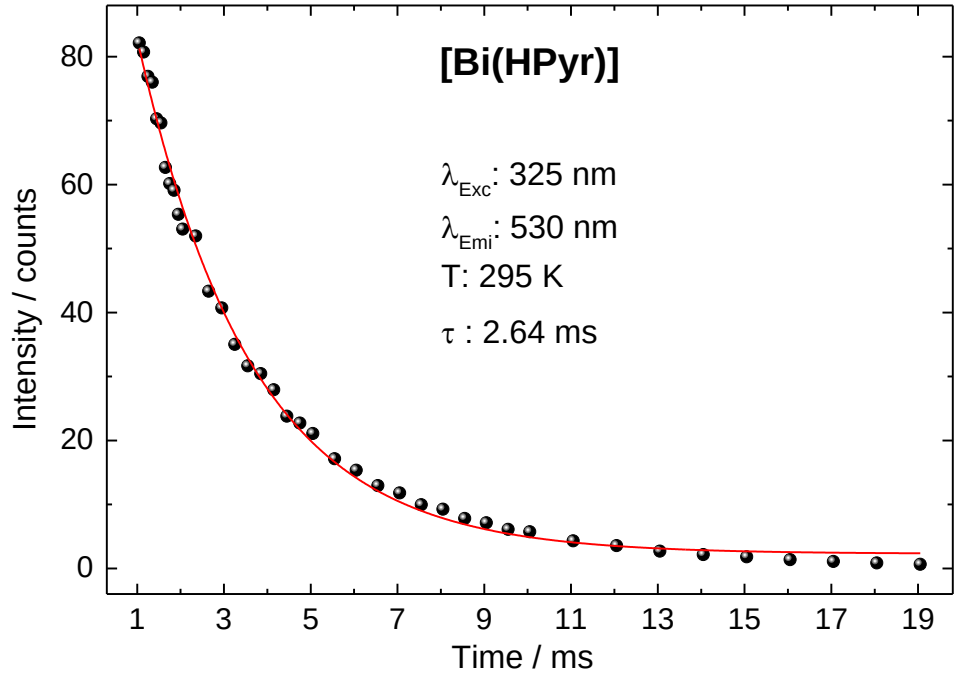

Fig. S10. First order fitting of the decay curve of nondoped [Bi(HPyr)] monitoring the emission in 530 nm at 295 K.

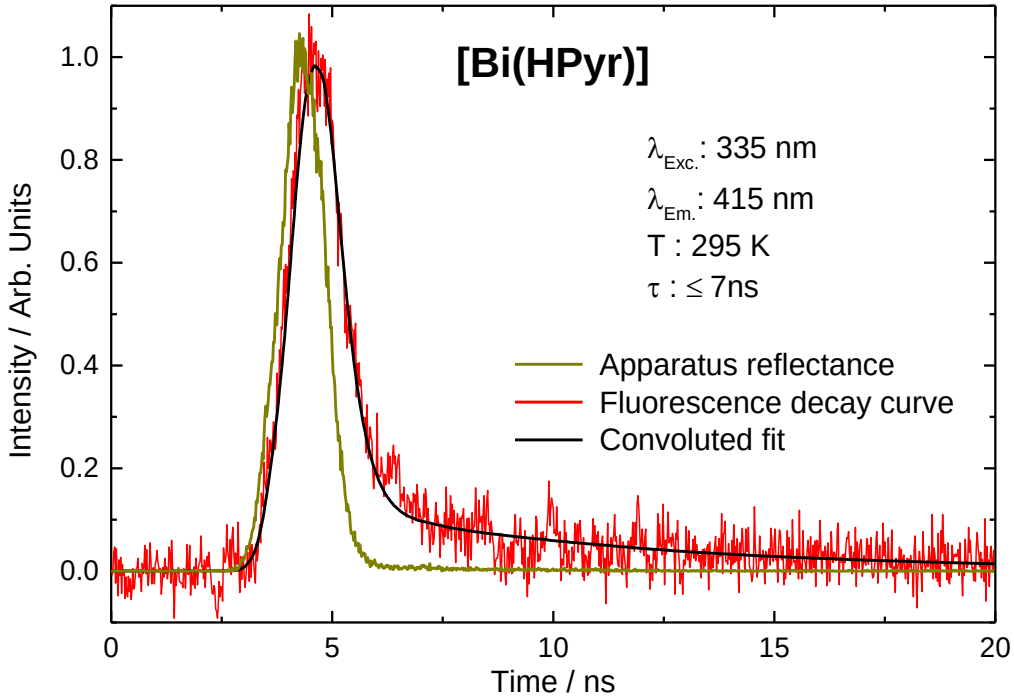

Fig. S11. Fluorescence decay curve of nondoped [Bi(HPyr)] at 295 K, in comparison with the apparatus reflectance. A convoluted fit (black curve) with a double exponential function yields two short time constants of $\tau_1 \sim 0.35$ ns and $\tau_2 \sim 7.0$ ns with a relative amplitude of $A_2/A_1 \sim 3.0$.

4. Luminescence tuning of the RE^{3+} double-doped [Bi(HPyr)] materials

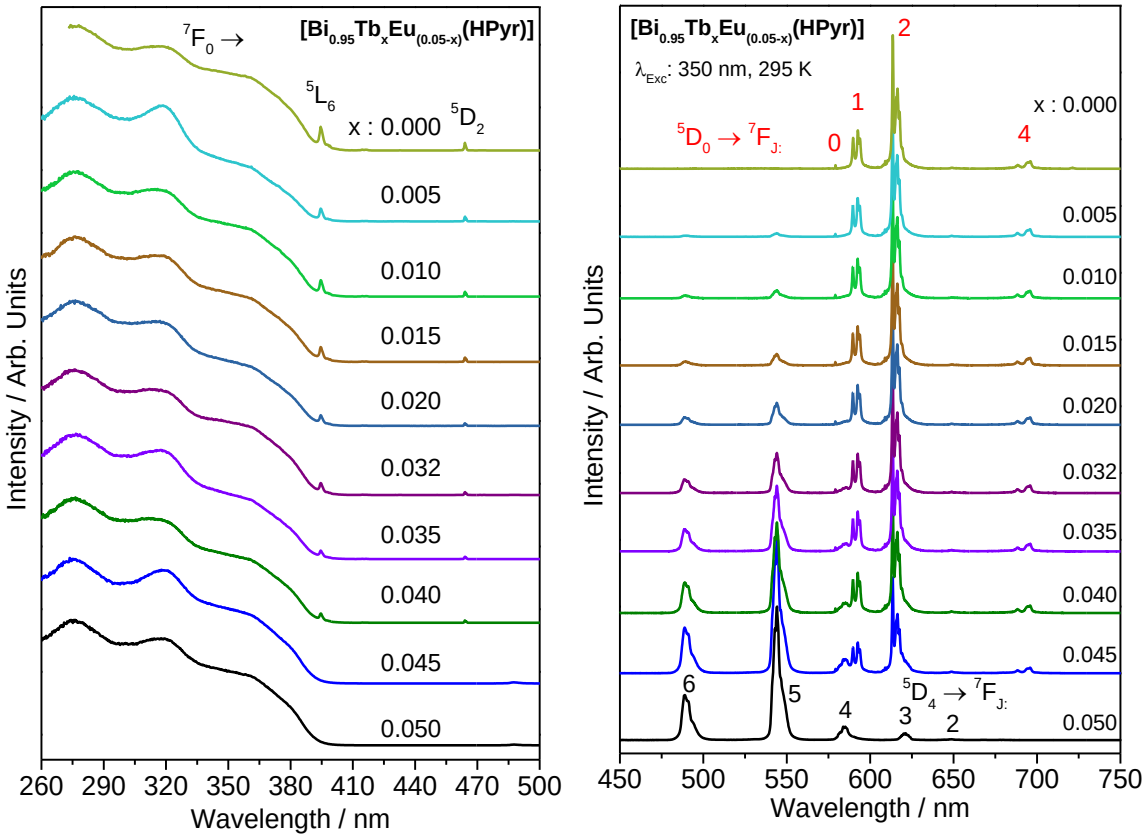

Fig. S12. Excitation spectra of the Tb^{3+}:Eu^{3+} double-doped [Bi(HPyr)] system, monitored at the maximum emission line of Tb^{3+} (λ_{emi} = 544.0 nm) or Eu^{3+} ions (λ_{emi} = 613.5 nm), respectively, at 295 K (Left). Emission spectra of the Tb^{3+}:Eu^{3+} double-doped [Bi(HPyr)] system, monitored following 350 nm excitation, at 295 K (Right).

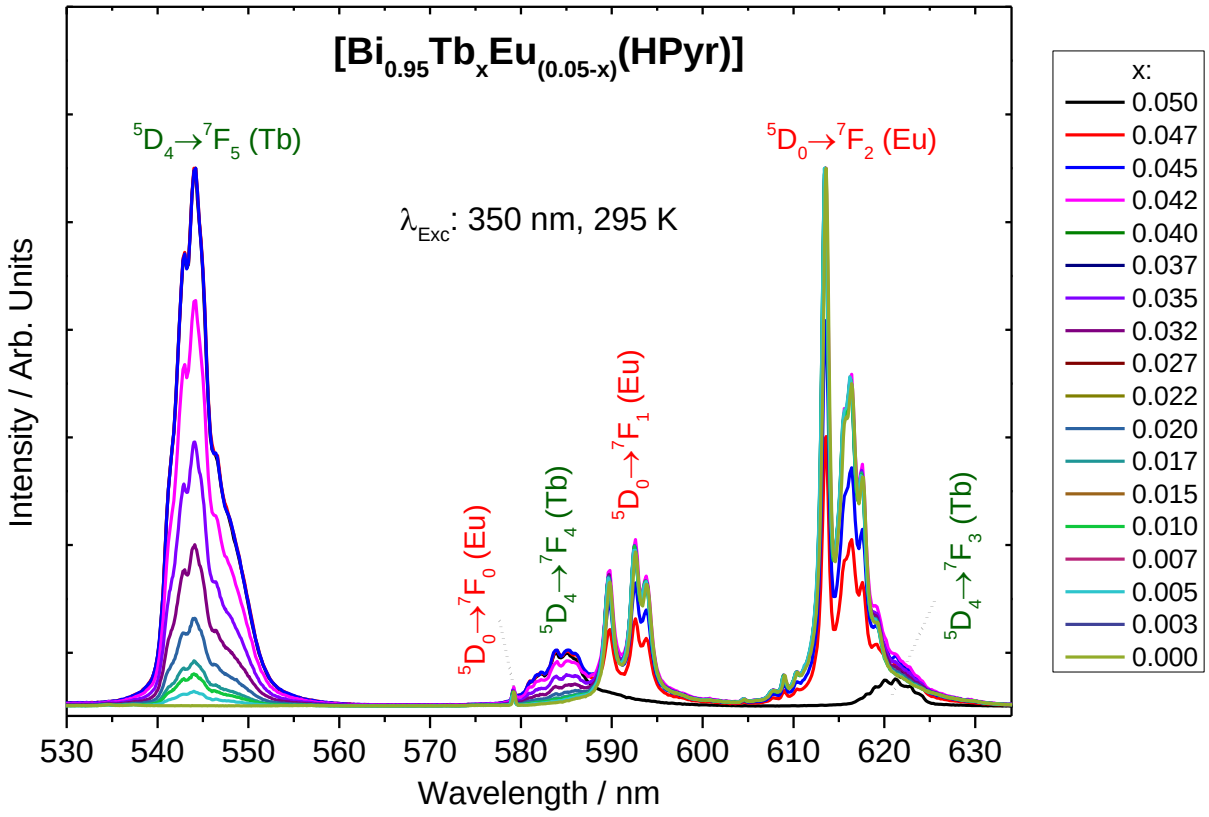

Fig. S13. Emission spectra of Tb^{3+}:Eu^{3+} double-doped [Bi(HPyr)] ($\lambda_{Exc.}$ 350 nm, 295 K), normalized with respect to the strongest emission peak.

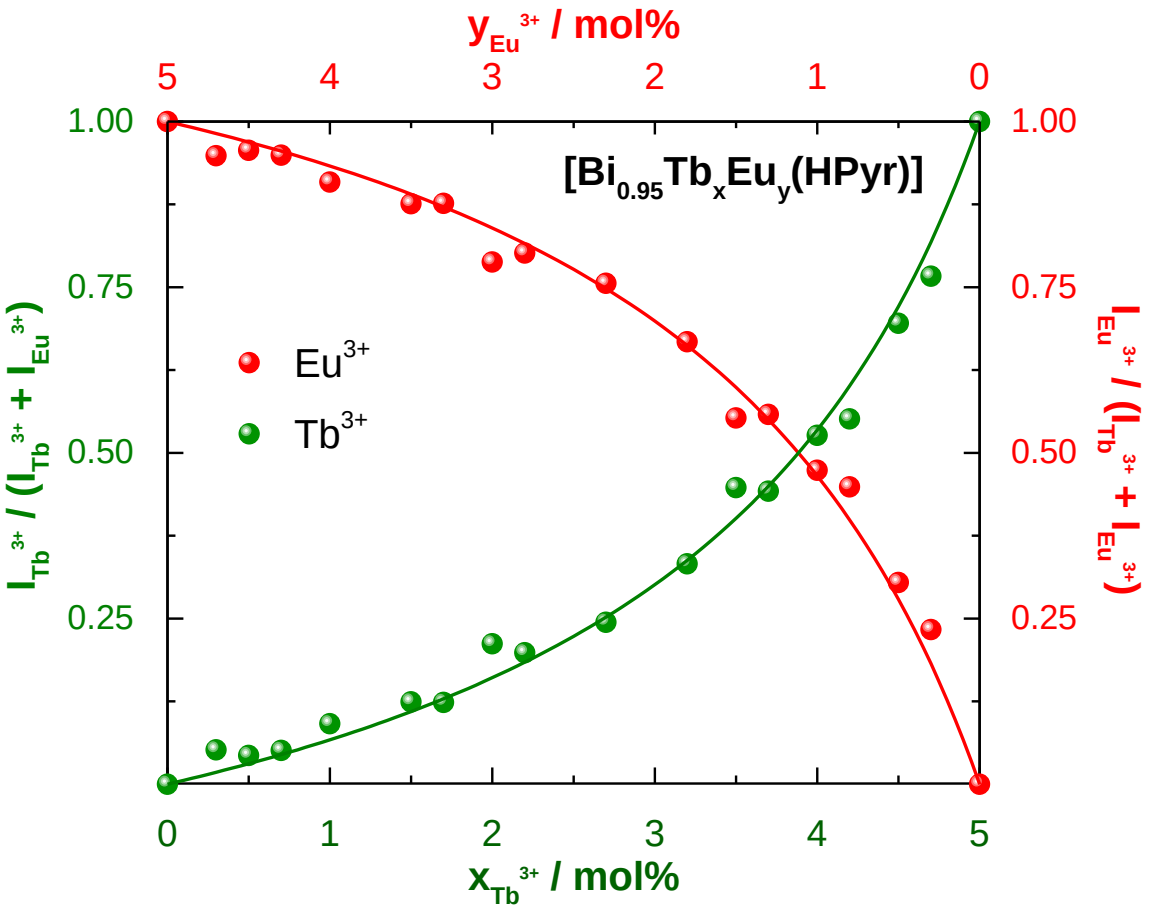

Fig. S14. Intensity ratios between emission bands of the Tb^{3+} and Eu^{3+} ions at different doping concentrations (0.3-5.0 mol%) in [Bi(HPyr)] matrix.

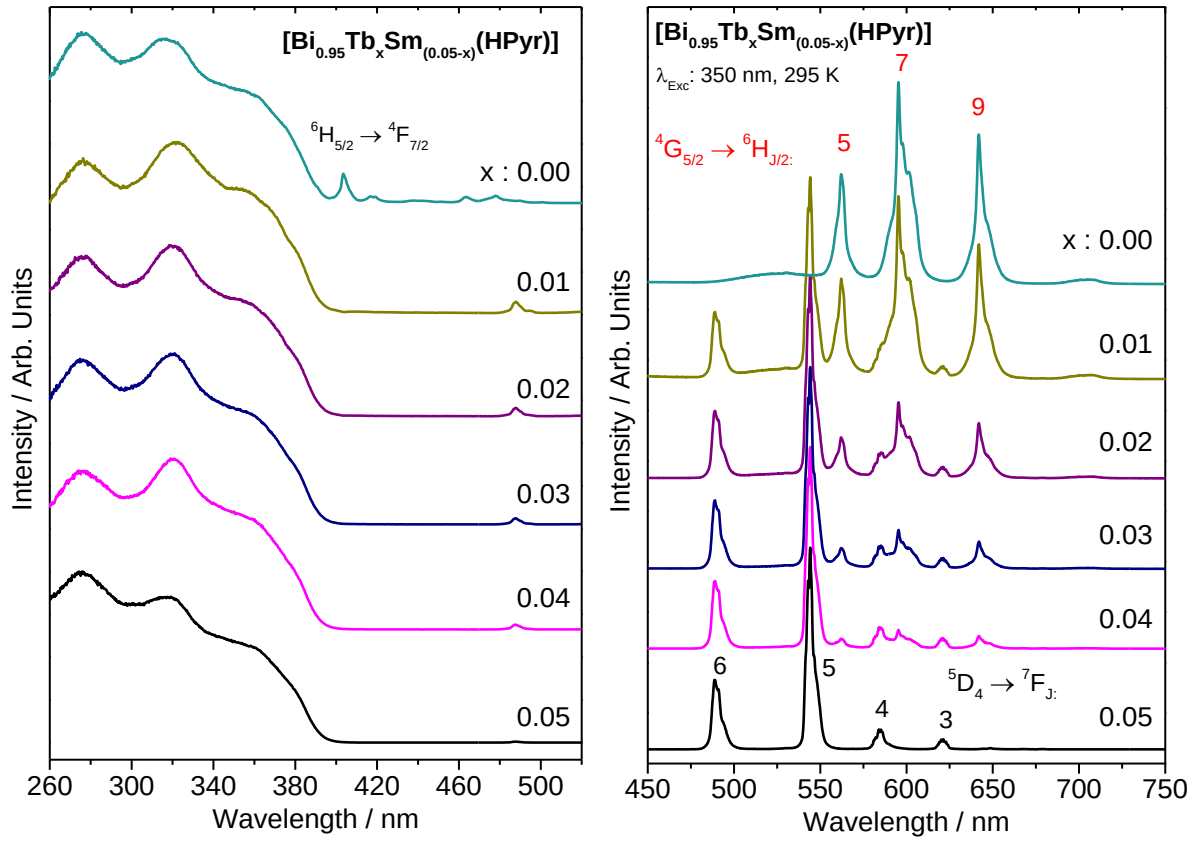

Fig. S15. Excitation spectra of the Tb^{3+}:Sm^{3+} double-doped [Bi(HPyr)] system, monitored at the maximum emission line of Tb^{3+} (λ_{emi} = 544.2 nm) or Sm^{3+} ions (λ_{emi} = 595.4 nm), respectively, at 295 K (Left). Emission spectra of the Tb^{3+}:Sm^{3+} double-doped [Bi(HPyr)] system, monitored following 350 nm excitation, at 295 K (Right).

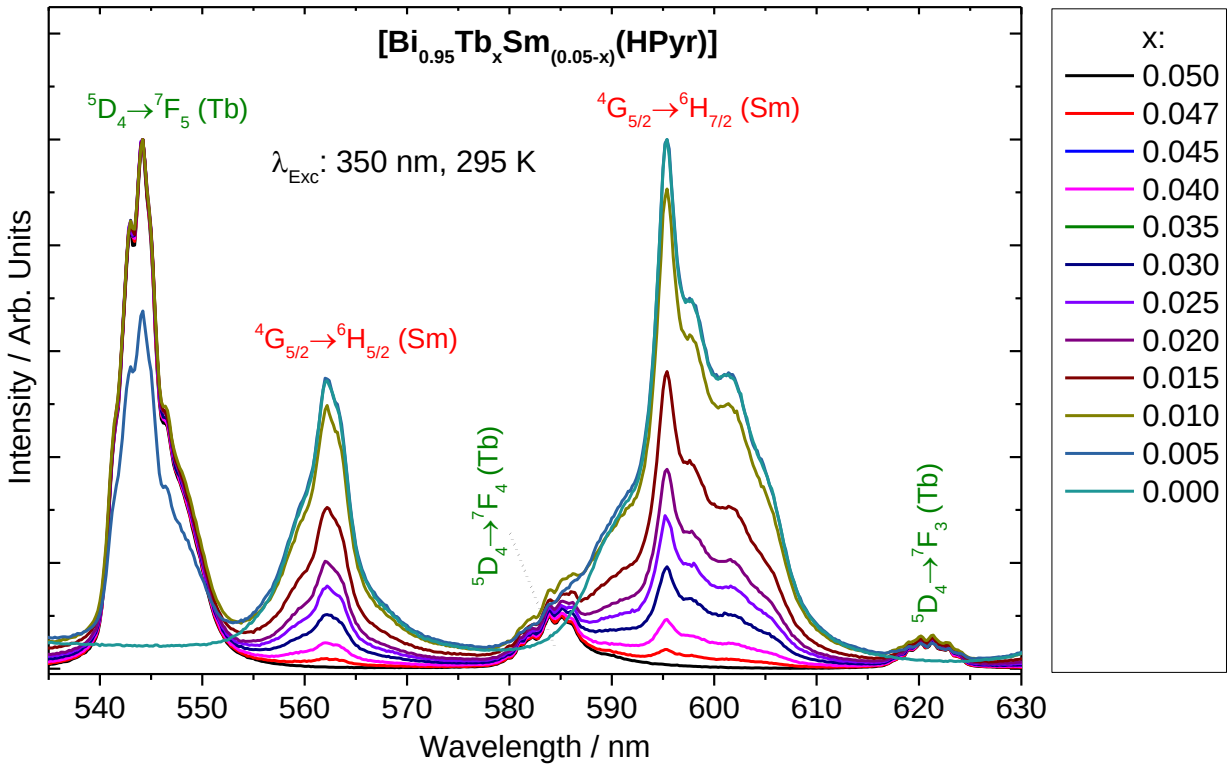

Fig. S16. Emission spectra of Tb^{3+}:Sm^{3+} double-doped [Bi(HPyr)] (λ_{Exc} 350 nm, 295 K), normalized with respect to the strongest emission peak.

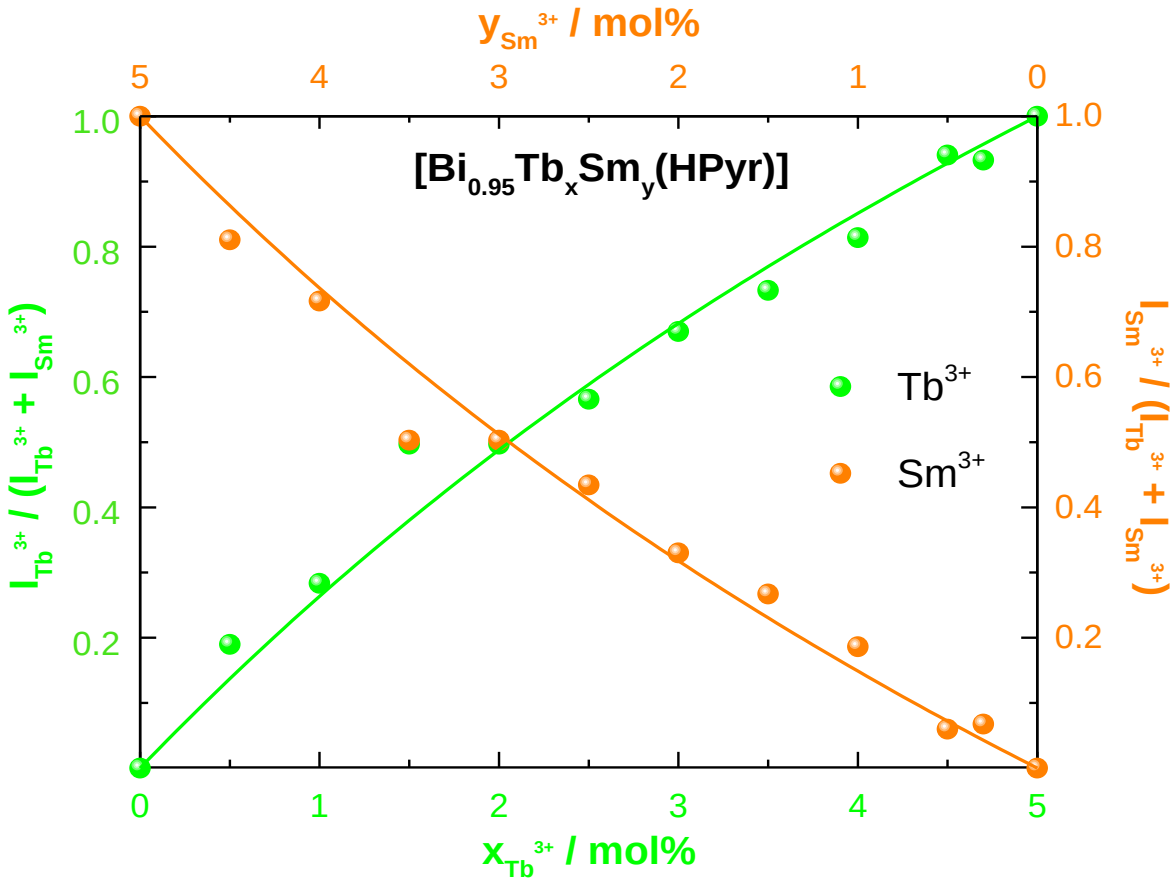

Fig. S17. Intensity ratios between emission bands of the Tb^{3+} and Sm^{3+} ions at different doping concentrations (0.5 – 5.0 mol%) in [Bi(HPyr)] matrix.

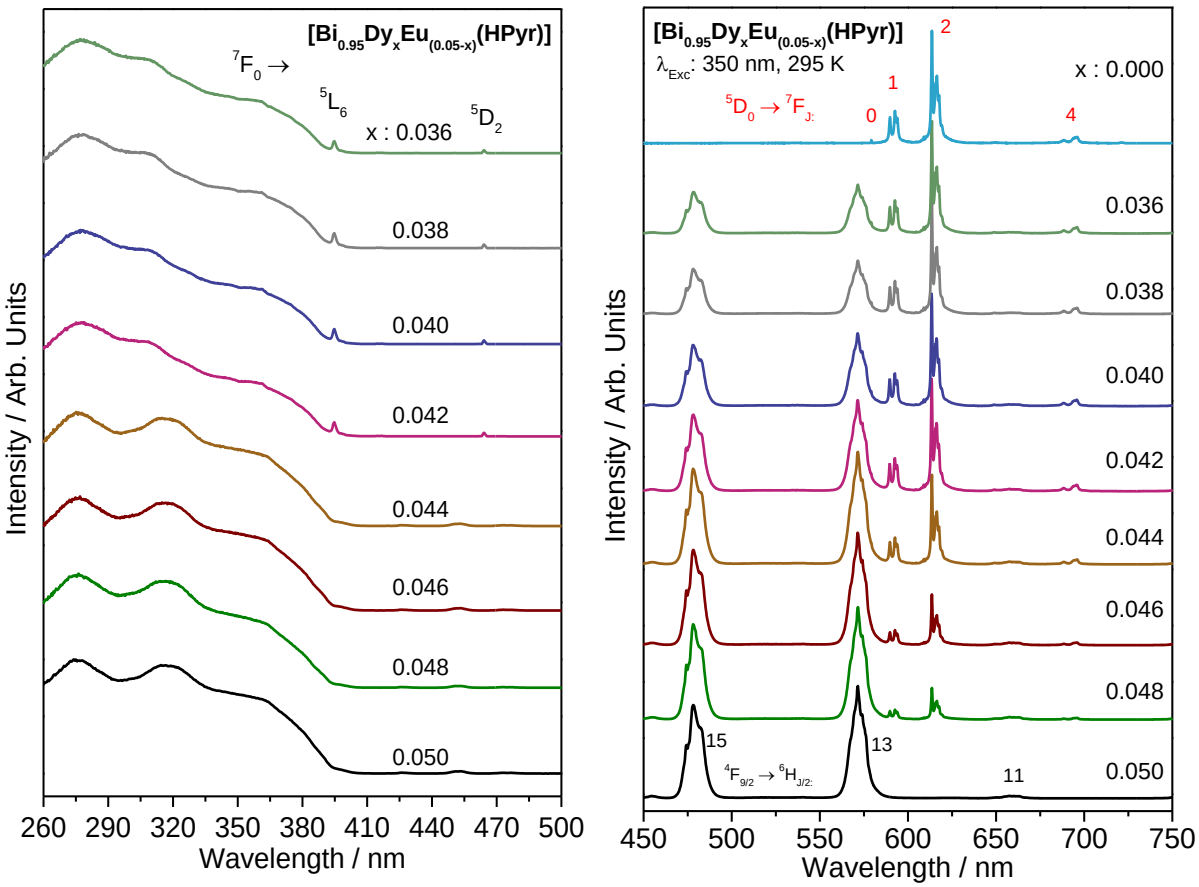

Fig. S18. Excitation spectra of the Dy^{3+}:Eu^{3+} double-doped [Bi(HPyr)] system, monitored at the maximum emission line of Dy^{3+} (λ_{emi} = 572.0 nm) or Eu^{3+} ions (λ_{emi} = 613.6 nm), respectively, at 295 K (Left). Emission spectra of the Dy^{3+}:Eu^{3+} double-doped [Bi(HPyr)] system, monitored following 350 nm excitation, at 295 K (Right).

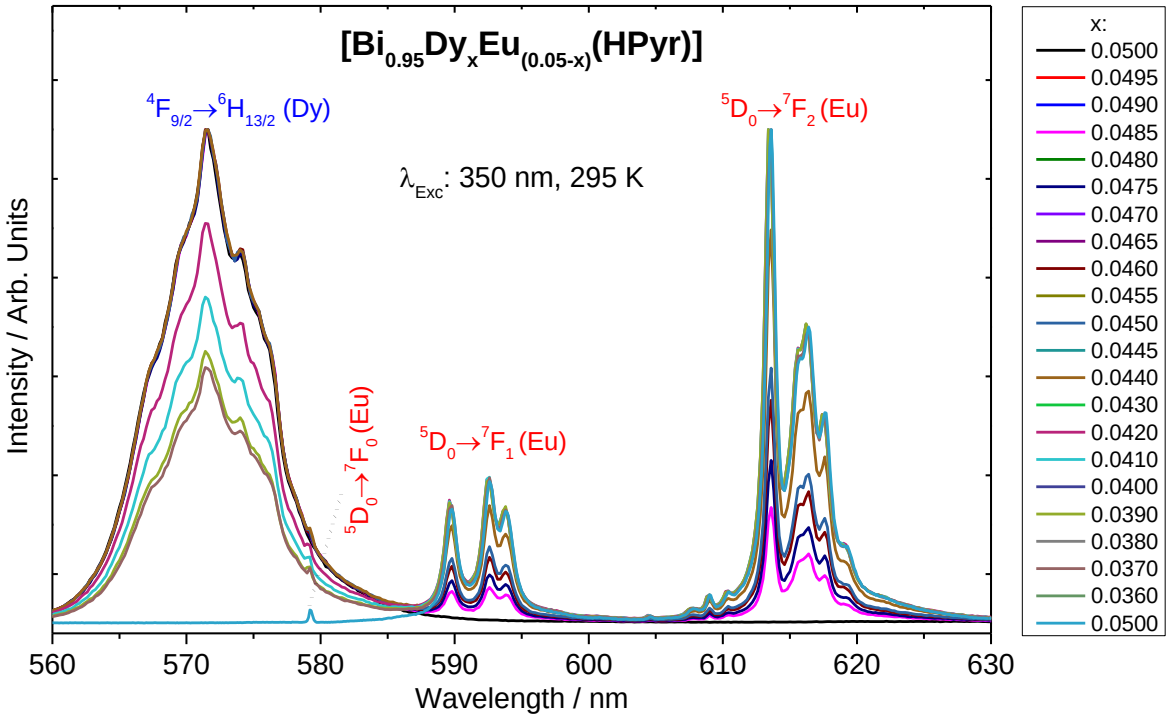

Fig. S19. Emission spectra of Dy^{3+}:Eu^{3+} double-doped [Bi(HPyr)] (λ_{Exc} 350 nm, 295 K), normalized with respect to the strongest emission peak.

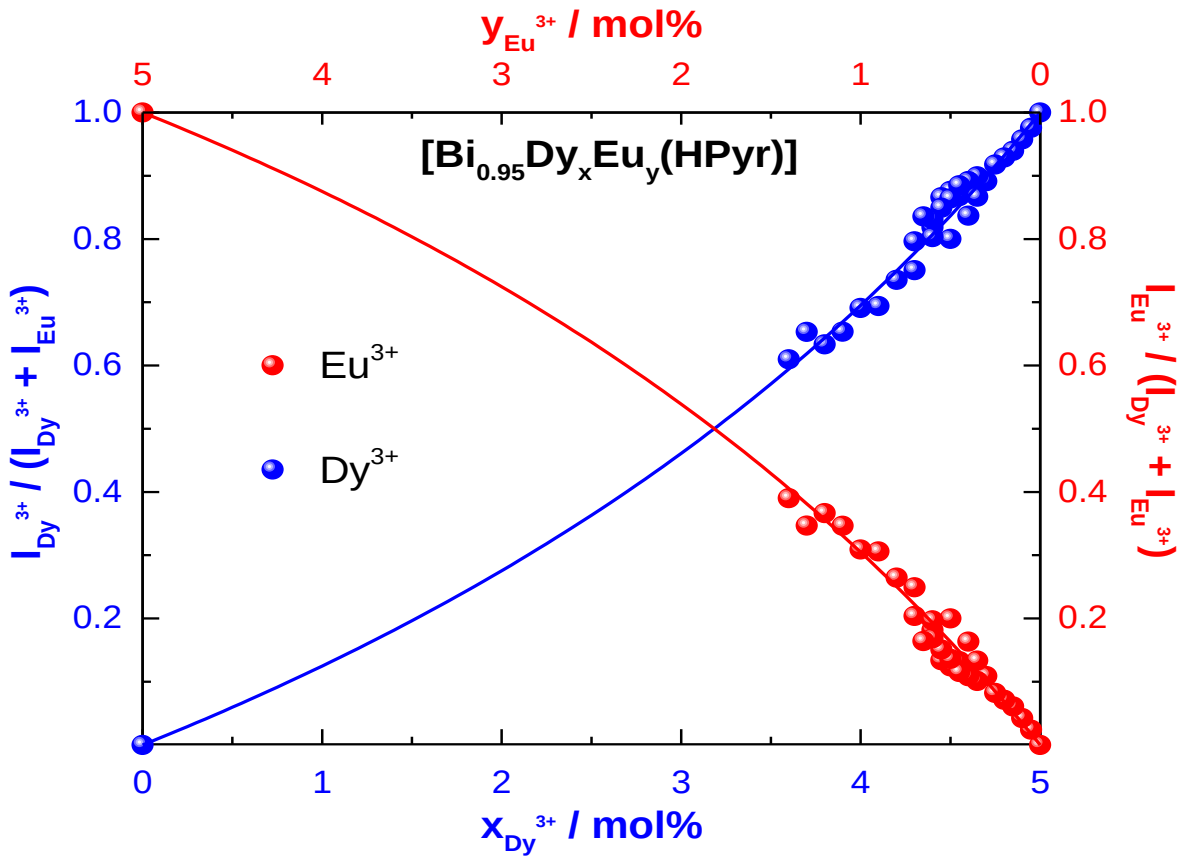

Fig. S20. Intensity ratios between emission bands of the Dy^{3+} and Eu^{3+} ions at different doping concentrations (3.6 – 5.0 mol%) in [Bi(HPyr)] matrix.

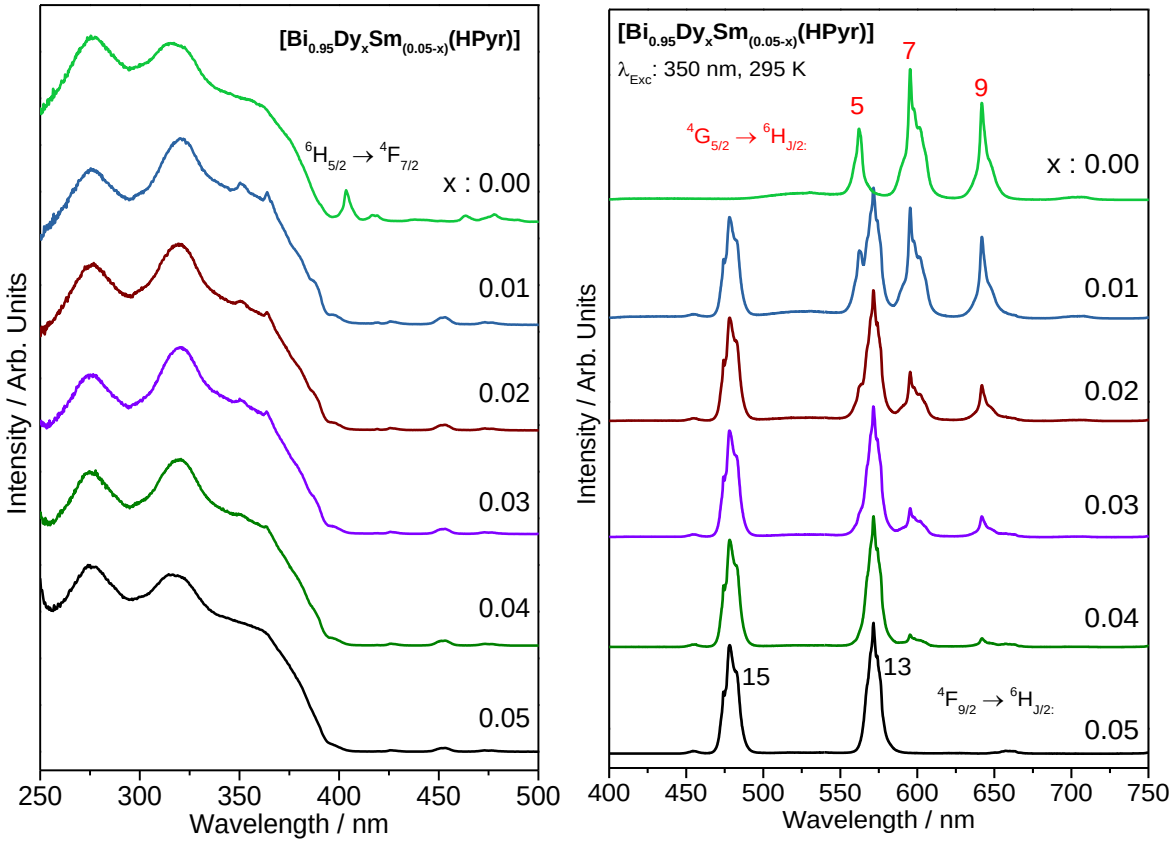

Fig. S21. Excitation spectra of the Dy^{3+}:Sm^{3+} double-doped [Bi(HPyr)] system, monitored at the maximum emission line of Dy^{3+} (λ_{emi} = 572 nm) or Sm^{3+} ions (λ_{emi} = 595 nm), respectively, at 295 K (Left). Emission spectra of the Dy^{3+}:Sm^{3+} double-doped [Bi(HPyr)] system, monitored following 350 nm excitation, at 295 K (Right).

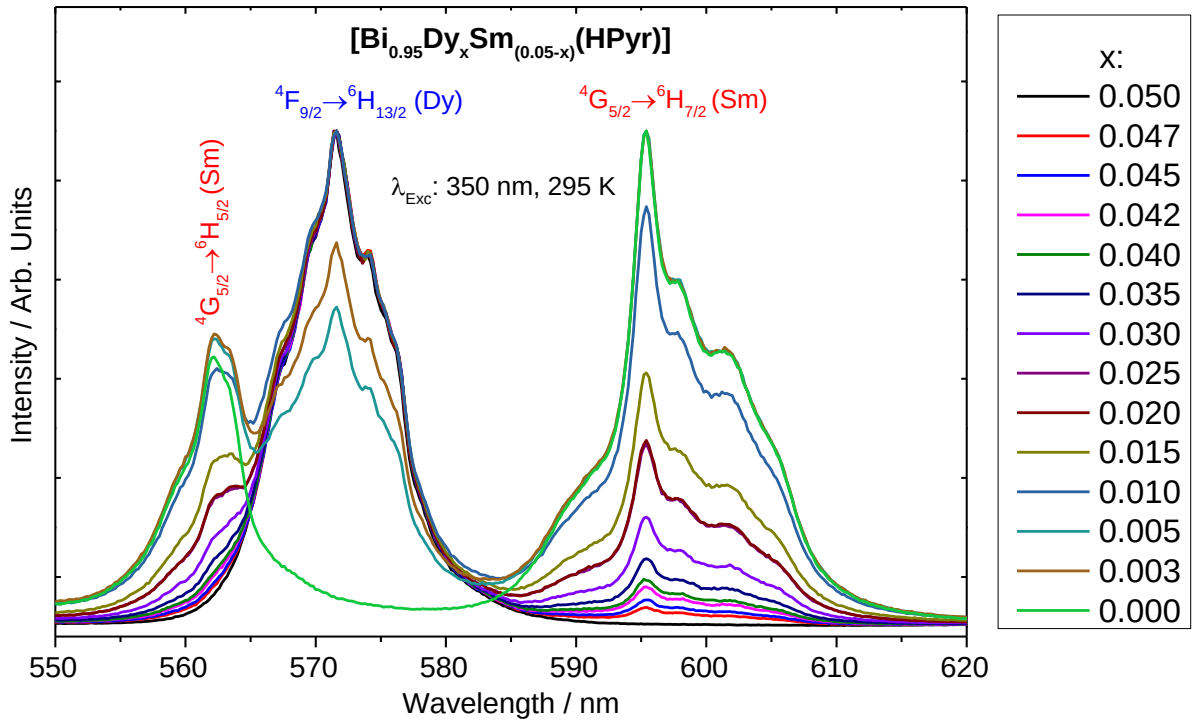

Fig. S22. Emission spectra of Dy^{3+}:Sm^{3+} double-doped [Bi(HPyr)] (λ_{Exc} 350 nm, 295 K), normalized with respect to the strongest emission peak.

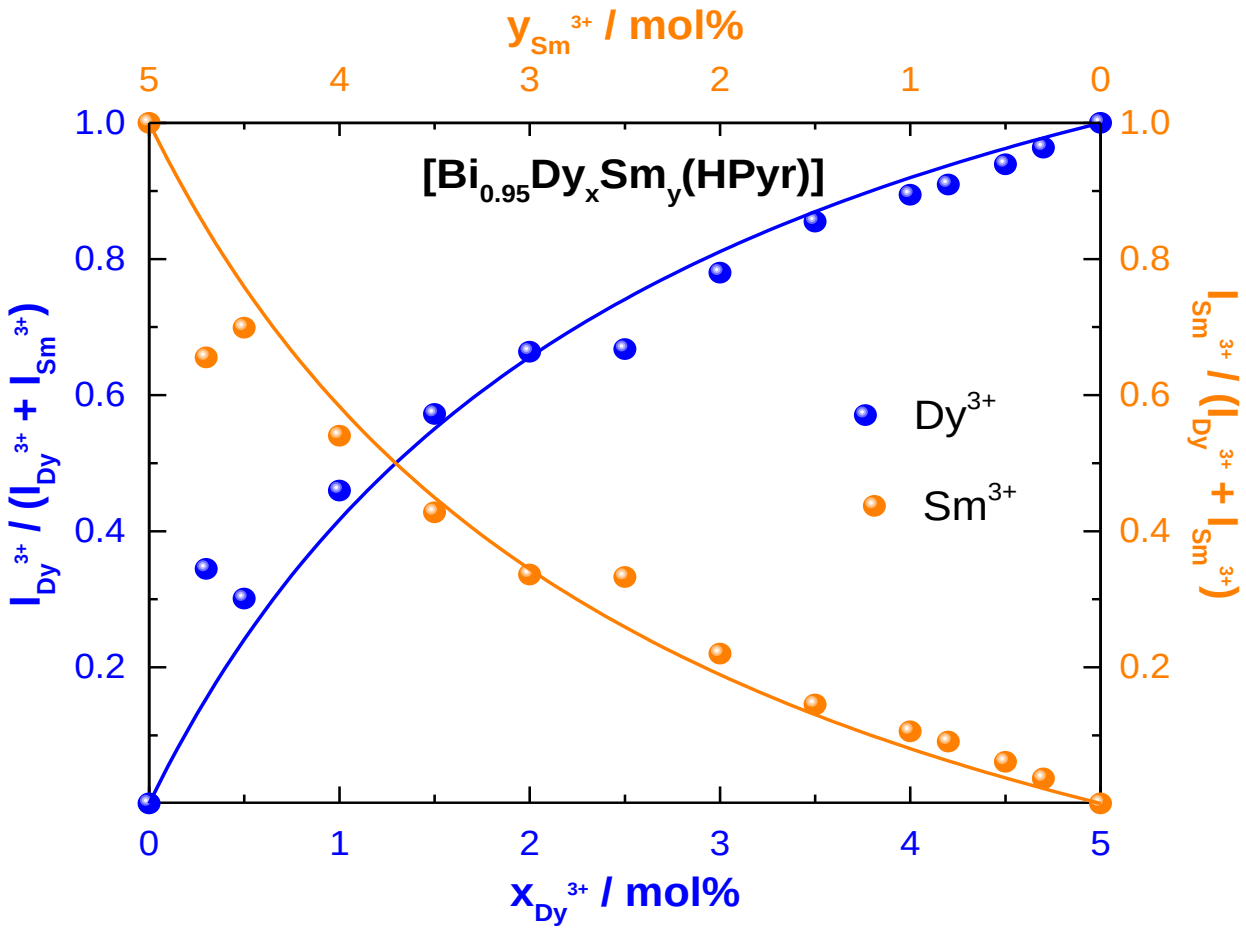

Fig. S23. Intensity ratios between emission bands of the Dy^{3+} and Sm^{3+} ions at different doping concentrations (0.3-5.0 mol%) in [Bi(HPyr)] matrix.

5. Decay curves of the RE^{3+} single- and double-doped [Bi(HPyr)] systems

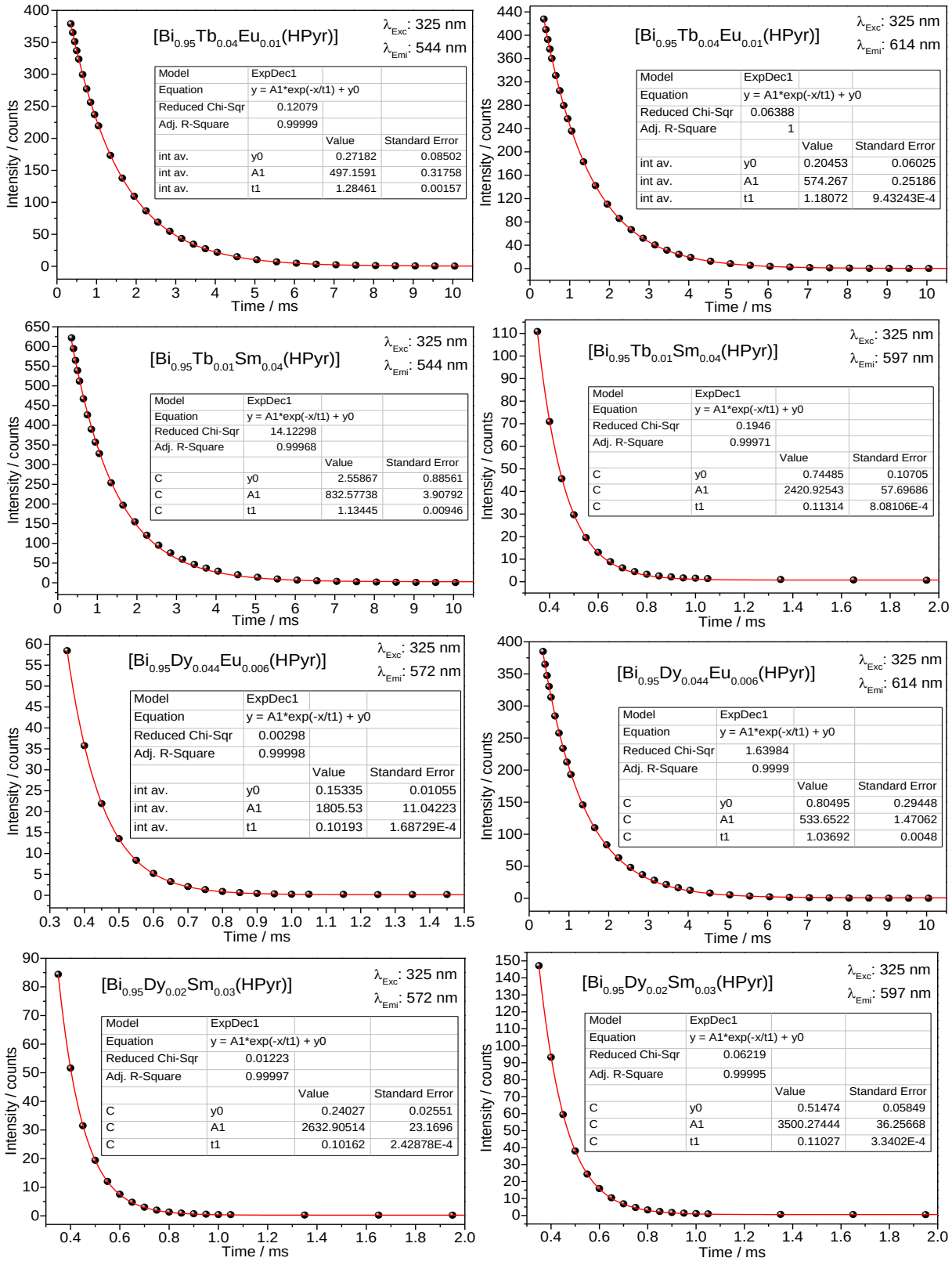

Fig. S24. First order fitting of the decay curves of RE^{3+} double-doped [Bi(HPyr)] systems, monitoring the maximum emission in each dopant ions (Tb^{3+}: 544 nm, Eu^{3+}: 614 nm, Dy^{3+}: 572 nm, Sm^{3+}: 597 nm) at 295 K.

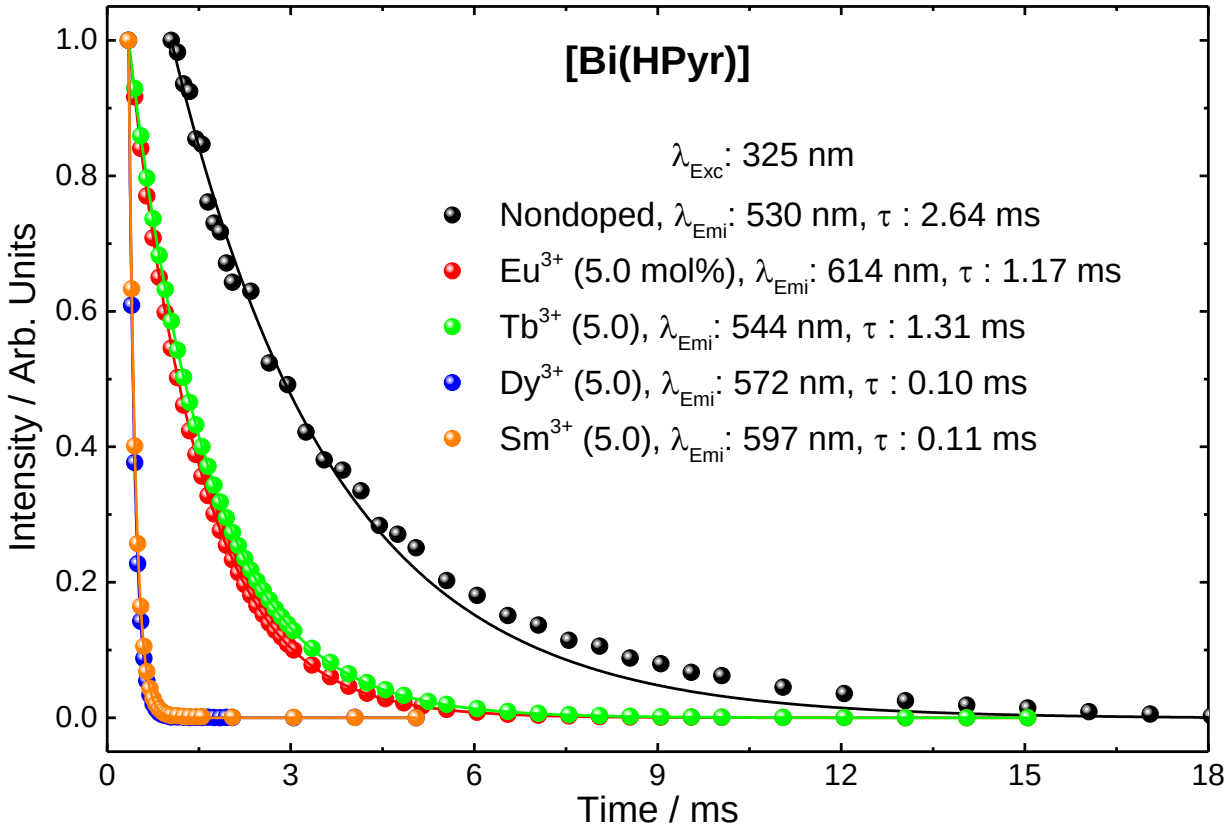

Fig. S25. First order fitting of the decay curve of nondoped and Sm^{3+}, Eu^{3+}, Tb^{3+} and Dy^{3+} single-doped [Bi(HPyr)] at 295 K, showing the monitored energies and lifetime values for the materials.

Table S9. Lifetimes values of the RE^{3+} doped [Bi(HPyr)] systems, obtained by a first order fitting in the decay curves shown in Fig. S23 and S24. Doping amounts are given in mol%.

RE^{3+} doping / mol%	τ_{Eu} / ms	τ_{Tb} / ms	τ_{Sm} / ms	τ_{Dy} / ms
Eu^{3+} (5.0 mol%)	1.167(1)			
Tb^{3+} (5.0)		1.310(1)		
Sm^{3+} (5.0)			0.1100(2)	
Dy^{3+} (5.0)				0.1019(2)
Tb^{3+} (4.0):Eu^{3+} (1.0)	1.181(1)	1.285(2)		
Tb^{3+} (1.0):Sm^{3+} (4.0)		1.134(9)	0.1131(8)	
Dy^{3+} (4.4):Eu^{3+} (0.6)	1.037(5)			0.1019(2)
Dy^{3+} (2.0):Sm^{3+} (3.0)			0.1103(3)	0.1016(2)

6. Chromaticity diagram and correlated color temperature (CCT)

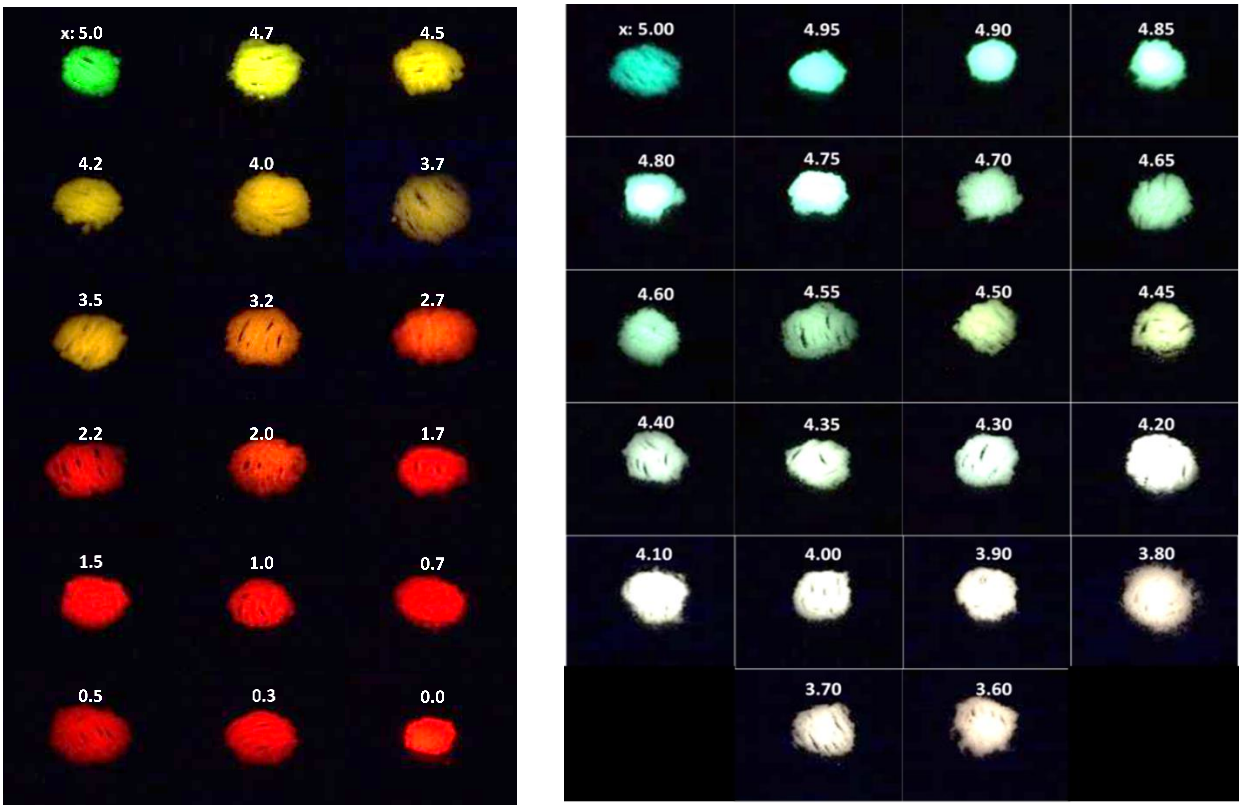

Fig. S26. xTb^{3+}:(5-x)Eu^{3+} double-doped [Bi(HPyr)] photographs under UV light (Left). xDy^{3+}:(5-x)Eu^{3+} double-doped [Bi(HPyr)] photographs under UV light (Right). Doping amounts are given in mol%.

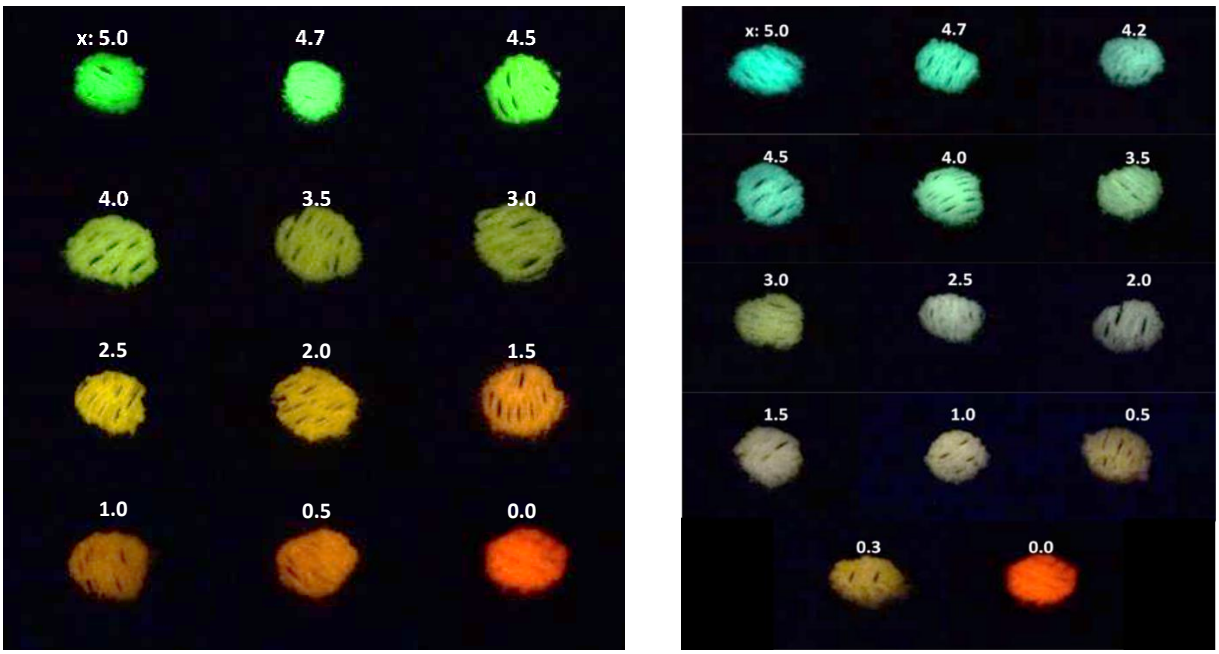

Fig. S27. xTb^{3+}:(5-x)Sm^{3+} double-doped [Bi(HPyr)] photographs under UV light (Left). xDy^{3+}:(5-x)Sm^{3+} double-doped [Bi(HPyr)] photographs under UV light (Right). Doping amounts are given in mol%.

Table S10. Color coordinates (*x,y*) used to generate the CIE diagram and CCT of the Dy^{3+}:Eu^{3+} double-doped [Bi(HPyr)] system.

$[Bi_{0.95}Dy_xEu_{(0.05-x)}(HPyr)]$	Color coordinates		CCT
	x	*y*	K
x: 0.0500	0.2909	0.3507	7456
0.0495	0.2985	0.3504	7066
0.0490	0.3035	0.3482	6834
0.0485	0.3098	0.3479	6524
0.0480	0.3146	0.3482	6291
0.0475	0.3177	0.3467	6153
0.0470	0.3283	0.3479	5674
0.0465	0.3237	0.3455	5883
0.0460	0.3284	0.3479	5669
0.0455	0.3312	0.3494	5547
0.0450	0.3381	0.3481	5263
0.0445	0.3401	0.3442	5174
0.0440	0.3499	0.3483	4801
0.0435	0.3500	0.3513	4812
0.0430	0.3591	0.3455	4453
0.0420	0.3842	0.3466	3653
0.0410	0.3993	0.3464	3239
0.0400	0.4015	0.3472	3193
0.0390	0.4138	0.3460	2892
0.0380	0.4260	0.3466	2647
0.0360	0.4327	0.3462	2518

Table S11. Color coordinates (*x,y*) used to generate the CIE diagram and CCT of the Dy^{3+}:Sm^{3+} double-doped [Bi(HPyr)] system.

$[Bi_{0.95}Dy_xSm_{(0.05-x)}(HPyr)]$	Color coordinates		CCT
	x	*y*	K
x: 0.050	0.2909	0.3507	7456
0.047	0.3004	0.3530	6940
0.045	0.3058	0.3557	6661
0.042	0.3121	0.3568	6363
0.040	0.3183	0.3601	6075
0.035	0.3266	0.3606	5731
0.030	0.3464	0.3464	4929
0.025	0.3757	0.3758	4120
0.020	0.3758	0.3747	4113
0.015	0.3977	0.3788	3579
0.010	0.4222	0.3854	3110
0.005	0.4676	0.3977	2484
0.003	0.4578	0.3983	2625
0.000	0.5422	0.4177	1929

Reference

1 M. Feyand, M. Köppen, G. Friedrichs and N. Stock, *Chem. Eur. J.*, 2013, **19**, 12537–12546.